DIFFRACTION AND SCATTERING
OF IONIZING RADIATIONS

Spectrometer of Synchrotron Radiation Based on Diffraction Focusing a Divergent Beam Formed by a Compound Refractive Lens

V. G. Kohn[a,b], I. A. Smirnova[c,*], I. I. Snigireva[d], and A. A. Snigirev[e]

[a] National Research Centre "Kurchatov Institute," Moscow, 123182 Russia

[b] Shubnikov Institute of Crystallography, Federal Scientific Research Centre "Crystallography and Photonics,"
Russian Academy of Sciences, Moscow, 119333 Russia

[c] Institute of Solid State Physics, Russian Academy of Sciences, Chernogolovka, Moscow oblast, 142432 Russia

[d] European Synchrotron Radiation Facility, Grenoble, France

[e] I. Kant Baltic Federal University, Kaliningrad, Russia

*e-mail: irina@issp.ac.ru

Received March 27, 2017

Abstract—The results of the first experimental realization of a spectrometer based on the effect of diffraction focusing of X rays by a flat single crystal are discussed. A secondary X-ray source with a relatively high angular divergence and small sizes was formed at the focus of a compound refractive lens having 50 beryllium biconcave elements with a curvature radius of 50 μm. The silicon spectrometer crystal was cut in the form of a wedge of variable thickness, oriented perpendicular to the diffraction plane. The reflection 111 was used for energies of 8.3 and 12 keV. To simulate the experiment, a computer program was developed, which takes into account accurately and for the first time the focusing of radiation by the lens and its subsequent diffraction in the crystal. A calculated curve for a monochromatic beam has made it possible to determine the monochromator spectrum with high resolution from experimental data for a polychromatic beam. It is shown that monochromator resolution increases with an increase in the distance from the compound refractive lens to the crystal.

INTRODUCTION

X-ray diffraction in a single crystal in the Laue geometry, where a reflected beam passes through a planar crystal, was experimentally investigated for the first time by Kato and Lang in 1959 [1]. Interference images under coherent illumination could be obtained using a narrow slit before a crystal, playing a role of a secondary radiation source with a small cross-sectional area. To describe theoretically this experiment, Kato developed a theory in the approximation of spherical incident wave [2, 3]. In this theory, it was suggested that the diffraction pattern on the output crystal surface arises in the Borrmann triangle, which is formed by the incident and reflected beam directions, and then is transferred intact to the detection plane. This method and theory, referred to as X-ray section topography, have been widely used for many years to study the quality of single crystals.

In 1977, Afanas'ev and Kohn [4] proposed a generalized theory of spherical wave diffraction, which explicitly takes into account the distance from the source to the detector. One of the main results of that study was the prediction of diffraction focusing of a divergent beam by a planar crystal. This effect was considered in more detail in [5]. It was experimentally verified in [6–9], where a crystal shaped as a wedge (i.e., with a variable thickness in the direction perpendicular to the diffraction plane) was used. In addition, an extraordinary interference pattern was revealed in the thin part of the wedge, which was referred to as the anomalous Pendellösung effect.

Twenty years after, the theory was formulated based on Fresnel propagators in [10], and a case of strong anisotropy was considered, where polychromatic focusing is implemented at different source–crystal and crystal–detector distances. Anomalous Pendellösung fringes were used in [11] to determine the local sample thickness.

A new-type spectrometer based on the diffraction focusing effect was proposed in theoretical study [12]. It allows one to record the entire energy spectrum of radiation at once (i.e., during one measurement) and with a high accuracy. This spectrometer was proposed to measure the spectrum of a single pulse of X-ray free-electron laser (XFEL) with a width of $\Delta E/E = 10^{-3}$ and an energy resolution of $\Delta E/E = 2 \times 10^{-6}$. A necessary condition for spectrometer operation is suf-
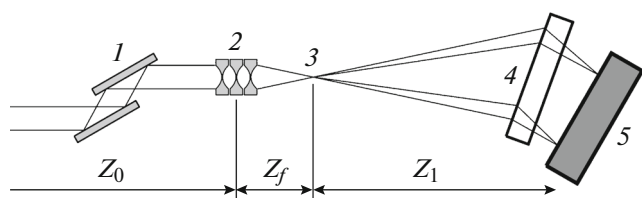
Fig. 1. Schematic of the experiment: a radiation beam is incident on monochromator *1* (having a vertical diffraction plane) and then on compound refractive lens *2*, located at a distance Z_0 from the source. The lens forms a secondary source of divergent radiation *3* at focal length Z_f; this radiation falls on spectrometer crystal *4* with a horizontal diffraction plane. Different monochromatic components, diffracting at different Bragg angles in the crystal, arrive at detector *5* at its different points. The distance Z_1 from the secondary source to the detector is approximately equal to the source−crystal distance.

ficiently high divergence of the X-ray beam incident on crystal.

The concept of this spectrometer is as follows. Diffraction focusing of reflected beam can be observed only under conditions of polychromatic focusing, when the source−crystal and crystal−detector distances are equal in symmetric case of diffraction. If the distance to the crystal greatly exceeds that to the detector, different monochromatic components are focused on the detector with different shifts. The shift is explained as follows: the crystal chooses the rays satisfying the Bragg condition from a divergent beam, whereas the Bragg angle depends on energy.

The resolution of this spectrometer depends on the quality of focusing the monochromatic component due to the effect of diffraction focusing. In addition, the beam size in the focus depends on not only the crystal properties but also on the source size, because the crystal does not change the source size in the focus. In other words, the spectrometer calls for a source with a high angular divergence and small sizes. However, neither XFEL sources nor synchrotron radiation (SR) sources satisfy these requirements. They are characterized by relatively large sizes and small angular divergence.

To solve this problem, it was proposed to use the secondary radiation source formed in the focus of a compound refractive lens [13, 14]. It is necessary to provide a large distance from the lens to the crystal and a small distance to the detector, which is also a problem to solve. If this condition is not satisfied, the spectrometer resolution is low.

It does not appear possible yet to use the new-type spectrometer on an XFEL. Hence, the first experimental test of this spectrometer was performed on a third-generation SR source; the results are reported below. SR is known to have a very wide spectrum; however, many SR stations are equipped with stationary monochromators, which sharply limit the emission spectrum; these devices are impossible to remove or replace. Therefore, we measured a relatively narrow spectrum formed by a monochromator.

An advantage of the new-type spectrometer for SR sources is the aforementioned possibility of recording the entire spectrum during one measurement with a short exposure (measurements on standard spectrometers are performed point by point for a long time). A spectrum can also be formed when radiation is absorbed or scattered by different materials, for example, in the vicinity of absorption jumps (EXAFS and XANES methods). A short measurement time allows one to analyze how a short-term impact affects a sample.

In this paper, we report experimental results in the form of section topograms, obtained from a secondary radiation source formed by a compound refractive lens. To describe the experiment, a special computer program was developed, which takes into account explicitly (for the first time) the focusing of radiation by a compound refractive lens and its subsequent diffraction in crystal. A numerical simulation of the experiment for a monochromatic beam made it possible to obtain a more detailed (as compared with direct measurements) monochromator spectrum.

EXPERIMENTAL

The experiment was performed on the ID06 station of third-generation SR source at the European Synchrotron Radiation Facility (ESRF) (Grenoble, France). A schematic of the experiment is shown in Fig. 1. The radiation source had the following vertical and lateral effective sizes: 30 and 900 μm, respectively. The primary slit was mounted at a distance of 27 m from the source and had a variable horizontal size and a fixed vertical size of 0.8 mm. A double-crystal monochromator Si(111) with a vertical diffraction plane was placed at a distance of 31 m from the source.

Rotating the monochromator, one could select a narrow spectrum in the vicinity of specified energy from a wide SR spectrum. Energies of 8.3 and 12 keV were used. A silicon spectrometer crystal was cut in the form of a wedge with a thickness varied along the vertical axis, the diffraction plane was horizontal, and the reflection 111 was applied. The secondary source was formed by a compound refractive lens, installed at a distance of 56 m from the source. The lens had 50 beryllium biconcave elements with a curvature radius of 50 μm, an aperture diameter of 450 μm, and a thickness of 1.05 mm [15].

For the aforementioned energies, the lens focal length Z_f, counted from the lens midplane, was calculated from the recurrence formulas [16, 17] to be 10.9 and 22.1 cm, respectively. A calculation using the thin lens formula, $R/(2N\delta)$, where R is the lens radius, N is the number of its elements, and $\delta = 1 - n$ (n is the real part of the refractive index), yields 10.1 and 21.2 cm, respectively. These values do not differ much from the results of more exact calculations. The effective-aper-

ture diameters are, respectively, 158 and 225 μm. These values are smaller than the geometric aperture because of the absorption of radiation at the edges of lens aperture; note that absorption is more pronounced at a lower energy.

The spectrometer crystal was located at different distances from the lens center, the largest of which was 147 cm. A 2D CCD detector was used to record reflected beam intensity; this detector provides a two-dimensional numerical array with an effective linear pixel size of 0.645 μm. The crystal was located close to the detector (the distance did not exceed 3 cm).

The first experiment was performed with an energy of 8.3 keV; the diffraction pattern was recorded at 50 points on the energy scale. The monochromator was rotated each time by such an angle as to increase energy by 1 eV. It turned out that a shift by 1 eV entirely displaced the diffraction pattern in an immobile detector by a distance of $x_{d\omega} = 11.7$ μm (18 pixels). For this energy, the Bragg angle $\theta_B = 13.74°$. One can estimate the difference between the distance L_0 from the secondary source at the lens focus to the crystal and the distance L_1 from the crystal to the detector using the formula [10]

$$\Delta L = L_0 - L_1 = \frac{x_{d\omega}}{\tan(\theta_B)(\Delta E/E)}. \tag{1}$$

Substituting the aforementioned values, we obtain $\Delta L = 39.8$ cm. This result is consistent with the distances at which the experiment was performed.

It is of interest to estimate the energy range δE that can be detected by a compound refractive lens at this distance. To this end, the effective aperture diameter must be divided by the focal length to obtain the angular aperture $\delta\theta$. In the case under consideration, $\delta\theta = 58 \times 10^{-4}/10.9 = 1.45 \times 10^{-3}$ rad. Correspondingly, $\delta E = E\delta\theta/\tan\theta_B = 49.4$ eV. This value is also in agreement with the experimental results. To measure a wider energy range, one needs a shorter focus lens.

At an energy of 12 keV, measurements were performed at different distances but without scanning energy. Figure 2 shows two experimental topograms (diffraction patterns) of a wedge-shaped silicon crystal for the reflection 111 at small (49 cm) and large (147 cm) distances. To recalculate the vertical coordinate of experimental topograms into crystal, one must know the thickness t_0 at which diffraction focusing of radiation is implemented. To this end, we will use the formula [4, 10]

$$t_0 = \frac{2|\chi_{rh}|\cos\theta_B}{\sin^2(2\theta_B)}L_t, \quad L_t = L_0 + L_1, \tag{2}$$

according to which t_0 is proportional to the total distance L_t. This is in agreement with the experiment, because the t_0 values in the topograms are 18.5 and 83.9 μm for the distances of 49 and 147 cm, respectively. The focusing efficiency is known to increase with an increase in the crystal thickness when the latter greatly exceeds the extinction length. According to the standard formulas, the extinction length for the Si reflection 111 is $\Lambda = 28.6$ μm. In the first case, $t_0 < \Lambda$; therefore, the focusing effect is practically absent. At the same time, the topogram contains pronounced interference fringes, which are described by the Kato theory; i.e., these are hyperbolic fringes, whose ends face the thicker part of the crystal.

In the second case, $t_0 \gg \Lambda$; therefore, one can observe focusing of a spherical wave in the topogram at a crystal thickness of about 90 μm. It can clearly be seen that in this case the image of a wedge-shaped crystal is very strongly smeared along the reciprocal lattice vector (x axis) in comparison with the first case. The image smearing is mainly determined by the limited spectral composition of the beam incident on the crystal.

The effect of image smearing clearly shows that the crystal works as a spectrometer. In the case of diffraction of a polychromatic X-ray beam, the monochromator crystal works as a prism, transforming a divergent white beam into a rainbow. The spectral composition of a diffracted wave can be estimated from the Bragg formula $\Delta\theta_B = (\Delta\lambda/\lambda)\tan\theta_B$ by equating $\Delta\theta_B$ to the angular monochromator size with respect to the radiation source. In the case under study, the monochromator was located at a distance of 31 m, and the vertical beam size before the monochromator was 0.8 mm. Dividing the latter value by the former, we find that $\Delta\theta_B = 2.58 \times 10^{-5}$ rad. Therefore, the relative spectral width of the beam after the monochromator is $\Delta\lambda/\lambda = 1.5 \times 10^{-4}$.

Then it is necessary to calculate again the angular divergence of radiation using the Bragg formula, but now for the spectrometer crystal. In the situation under consideration, the crystals are identical, and the same reflection is used; therefore, it is sufficient to know the angular monochromator size. The spatial image smearing, related to the limited spectral composition of the beam incident on the spectrometer crystal, can be estimated from a simple formula: $\Delta x = \Delta L\Delta\theta$. In the first case, $\Delta L = 27$ cm; therefore, $\Delta x = 6.9$ μm. In the second case, $\Delta L = 125$ cm and $\Delta x = 32.3$ μm. Thus, at a larger difference of distances ΔL, the image smearing along the reciprocal lattice vector is larger. This factor increases the spectrometer sensitivity, which is determined by the ratio of the width of a beam focused due to the effect of diffraction focusing in the case of monochromatic radiation to the degree of image smearing for the spectrum of a real beam incident on the spectrometer.

THEORY

It is known that the monochromators used on SR sources do not change the beam direction; i.e., a beam is reflected twice in the forward and backward direc-
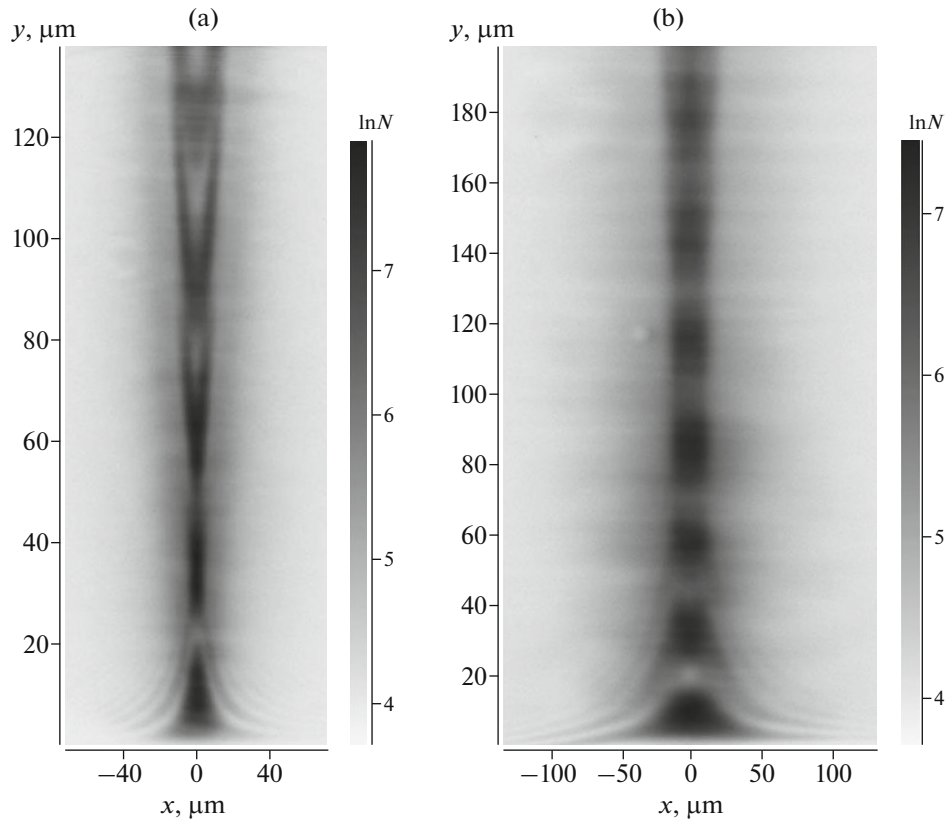
Fig. 2. Experimental topograms of a wedge-shaped silicon crystal (reflection 111) at lens–crystal distances of (a) 49 and (b) 147 cm. The crystal thickness is plotted on the y axis. A logarithm of the number of pulses in the CCD detector is shown on the gray shade scale.

tions. If experimental results are simulated within the schematic shown in Fig. 1, the monochromator can be disregarded, because it only slightly limits the angular divergence of radiation. However, if the width of the beam illumination region before the compound refractive lens exceeds the lens effective aperture, the monochromator in no way affects the diffraction pattern formed by the crystal.

Let us consider an individual monochromatic radiation harmonic, which is coherent and is described by Maxwell equations. Taking into account that the diffraction pattern depends on only the total distance between the lens and detector, we assume for simplicity that the detector is located directly behind the crystal. In this case, the electric field amplitude on the detector can be written in the form

$$E(x) = \int dx_1 P_C(x - x_1)$$
$$\times \int dx_2 P(x_1 - x_2, z_1) T(x_2) P(x_2 - x_0, Z_0),$$
(3)

where Z_0 is the distance from the point source to the lens; $z_1 = Z_f + Z_1$ is the distance from the lens to the detector (Fig. 1); the Fresnel propagator

$$P(x, z) = (i\lambda z)^{-1/2} \exp\left(i\pi \frac{x^2}{\lambda z} \right) \tag{4}$$

is the spherical wave component along the x direction in the paraxial approximation; and the crystal propagator

$$P_C(x) = \int \frac{dq}{2\pi} \exp(iqx) P_C(q) \tag{5}$$

is a Fourier transform of the plane-wave reflection amplitude $P_C(q)$, whose direction differs from the Bragg direction by the angle $\theta = q/K$ ($K = 2\pi/\lambda$). The formulas for calculating $P_C(q)$ can be found in [10].

In contrast to problem [10], an incident wave in the case under consideration is modified by a compound refractive lens. Within the thin lens approximation, it is presented by the transmission function

$$T(x) = \exp\left(i\pi \frac{x^2}{\lambda F} [1 - i\gamma] \right),$$
$$F = \frac{R}{2N\delta}, \quad \gamma = \frac{\beta}{\delta}. \tag{6}$$

Here, β is the imaginary part of complex refractive index $n = 1 - \delta + i\beta$. The influence of the source size on the diffraction pattern is taken into account

through the coordinate x_0, which describes a lateral shift of a point source from the optical axis.

The radiation intensity $I(x) = |E(x)|^2$ is experimentally measured. To calculate the intensity from formula (3), a computer program was developed using properly interpreted language ACL. ACL interpreter is a Java program, which is freely available in the Internet, along with the language description [18]. This program makes it possible to calculate the distribution intensity in the case of diffraction of monochromatic radiation from a point source for crystals of arbitrary thickness and construct a two-dimensional intensity map for a wedge-shaped crystal.

Figure 3 shows two intensity distribution curves at the aforementioned parameters, i.e., for a beryllium compound refractive lens with an effective curvature radius $R_0 = R/N = 1$ μm, radiation energy 12 keV, 98-μm-thick Si crystal, reflection 111, $Z_0 = 5600$ cm, and $z_1 = 147$ cm. These curves have different point source coordinates: $x_0 = 0$ and 450 μm. One can see that a displacement of a point source by 450 μm (half source size in the experiment) shifts the curve as a whole to the opposite side by -1.75 μm.

This result shows that the crystal responds to the secondary source, located at the lens focus. A known property of Fresnel propagator is that a convolution of two propagators located at distances Z_f and Z_1 is equal to the Fresnel propagator located at the total distance $z_1 = Z_f + Z_1$. Taking into account this property, the crystal response can mathematically be presented in the form

$$E(x) = \int dx_1 P_C(x - x_1) \int dx_2 P(x_1 - x_2, Z_1) B(x_2, x_0), \quad (7)$$

$$B(x, x_0) = \int dx_1 P(x - x_1, Z_f) T(x_1) P(x_1 - x_0, Z_0). \quad (8)$$

The function $B(x, x_0)$ describes the radiation field at the lens focus. Substituting (4) and (6), we obtain

$$B(x, x_0) = \frac{A(x, x_0)}{i\lambda [Z_f Z_0]^{1/2}} \int dx_1 \\ \times \exp\left(-i2\pi \frac{(x - x_0')}{\lambda Z_f} x_1 - \frac{\pi\gamma}{\lambda F} x_1^2\right), \quad (9)$$

where

$$A(x, x_0) = \exp\left(-i\pi\left[\frac{x^2}{\lambda Z_f} + \frac{x_0^2}{\lambda Z_0}\right]\right), \\ x_0' = -x_0 \frac{Z_f}{Z_0}. \quad (10)$$

Here, the relation $1/Z_f = 1/F - 1/Z_0$ is used.

Having calculated the integral, we arrive at the final relation

$$B(x, x_0) = \frac{A(x, x_0)}{iC_2} G(x - x_0', \sigma), \quad (11)$$
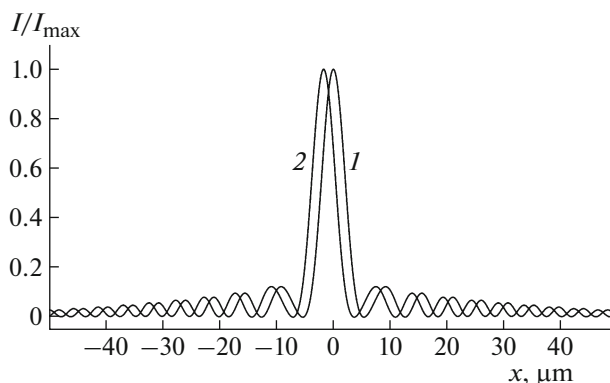

Fig. 3. Theoretical curves of diffracted radiation intensity for two point-source coordinates $x_0 = $ (*1*) 0 and (*2*) 450 μm and crystal thickness of 98 μm.

where

$$C_2 = \left(\frac{C_1}{1 - C_1}\right)^{1/2}, \quad C_1 = 1 - \frac{F}{Z_0}, \quad \sigma = \frac{1}{C_1}\left(\frac{\lambda F\gamma}{2\pi}\right)^{1/2}, \\ G(x, \sigma) = \frac{1}{\sigma(2\pi)^{1/2}} \exp\left(-\frac{x^2}{2\sigma^2}\right). \quad (12)$$

Thus, the amplitude of radiation field distribution at the focus in the horizontal direction is proportional to a Gaussian with a full width at half maximum $w = 2.355\sigma$. When a source is displaced by a distance x_0, the Gaussian shifts as a whole by a distance x_0'.

At an accuracy at the level of constant phase factor M, which does not affect the intensity, we have

$$B(x, x_0) = B(x - x_0', 0) M \exp\left(i\pi\frac{2xx_0'}{\lambda Z_f}\right). \quad (13)$$

Hence, at a lateral shift of point source by a distance x_0, the radiation field at the focus is not only shifted as a whole by a distance x_0' but also gains an additional phase factor, which differently depends on x. Note that, when integrating, the coordinate x differs from x_0' only within the focus diffraction width w.

If the focus diffraction limited width is small, the phase factor, remaining almost constant at relatively small displacements x_0, can be neglected. Correspondingly, using the property of convolutions in (7), we find that the diffraction pattern shifts as a whole by a distance x_0', in correspondence with numerical calculations. However, this result is not universal. It is valid only when the beam is sufficiently strongly focused by lens.

An accurate calculation within the program shows that the diffraction focusing peak is displaced at any shift of the source, and its maximum value decreases. If the peak height at zero shift is assumed to be unity, shifts by 5, 10, and 15 mm reduce the peak height to
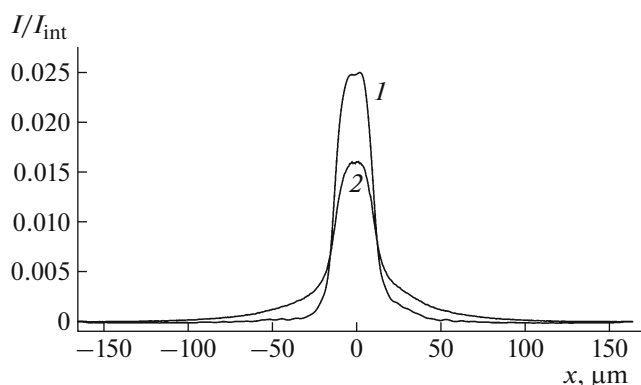
Fig. 4. Monochromator spectrum (*1*) calculated from experimental intensity curve (*2*) at a crystal thickness of 98 μm. The curves are normalized so that the integral of the functions is unity.

0.95, 0.85, and 0.69 respectively. The peak height decreases due to the presence of phase factor in (13), which does not play any role when the intensity is measured directly at the lens focus.

DETERMINATION OF MONOCHROMATOR SPECTRUM

SR is known to be a set of fairly short pulses. If the measurement time greatly exceeds the pulse duration, one can show that the phase relations between different monochromatic components of radiation are lost. In other words, the experimental intensity of polychromatic radiation is the sum of monochromatic harmonic intensities.

If the photon energy changes in a narrow range, the diffraction pattern is retained as a whole; it is only the Bragg angle that changes. As can be seen in Fig. 3, this change leads to a lateral shift x_ω of the diffraction pattern recorded by the detector. The experimentally measured radiation intensity $I_{ep}(x)$ for a specified crystal thickness is a convolution:

$$I_{ep}(x) = \int dx_\omega I_{em}(x - x_\omega) S(x_\omega), \qquad (14)$$

where $I_{em}(x)$ is the experimental intensity of monochromatic radiation and $S(x_\omega)$ is the emission spectrum formed by the monochromator. In turn, the intensity $I_{em}(x)$ is a convolution

$$I_{em}(x) = \int dx_0 I_{emp}(x - x_0') I_s(x_0'), \qquad (15)$$

where $I_{emp}(x)$ is the monochromatic radiation intensity from a point source and $I_s(x)$ is a function of secondary source brightness. It is only the intensity $I_{ep}(x)$ that is directly measured. At the same time, the intensity $I_{emp}(x)$ can be calculated using the computer program. Correspondingly, one can calculate the intensity $I_{em}(x)$ from formula (15), approximating the function $I_s(x)$ by a Gaussian. The full width at half

maximum (FWHM) of Gaussian distribution is equal to the source image size at the focus.

It was suggested in [12] that the FWHM of the intensity peak described by the function $I_{em}(x)$ under conditions of diffraction focusing is fairly small, whereas the FWHM $S(x_\omega)$ is, in contrast, large. Replacing approximately $I_{em}(x - x_\omega)$ in (14) with δ function, we obtain $S(x) = I_{ep}(x)$. In other words, the experimental curve yields at once a spectrum with a certain accuracy.

The aforementioned condition is not satisfied in our study. The monochromator forms a fairly narrow emission spectrum, whose width is not much larger than the peak width $I_{em}(x)$. Let us choose the crystal thickness $t = 98$ μm, at which the peak of function $I_{emp}(x)$ has a minimum FWHM $T_{emp} = 4.5$ μm. Correspondingly, the FWHM of the peak in the curve of secondary source brightness $I_s(x)$ is $T_{ss} = 3.5$ μm; i.e., the peak FWHM $I_{em}(x)$ can roughly be estimated as $T_{em} = ((T_{emp})^2 + (T_{ss})^2)^{1/2} = 5$ μm. At the same time, as follows from the experiment, the peak width $I_{ep}(x)$ for this crystal thickness is $T_{ep} = 25.8$ μm; i.e., is much larger.

Therefore, to perform a rough estimation, one can assume that $S(x) = I_{ep}(x)$. To obtain a more accurate result, it is necessary to calculate convolution (15) and then calculate the function $S(x)$ from Eq. (14) using double Fourier transform. Figure 4 shows the thus calculated monochromator spectrum (i.e., the function $S(x)$). The spectrum is normalized to unit area. This figure shows also an experimental curve $I_{ep}(x)$ subjected to the same normalization. As follows from Fig. 4, the shape of the monochromator spectrum resembles the Bragg reflection curve for two crystals; i.e., the spectrum is described by a Π-shaped function with slightly distorted tails. The calculation of the spectrum from the convolution significantly reduces the relative error in determining this spectrum in comparison with the initial experimental curve.

CONCLUSIONS

It was experimentally shown that the new-type spectrometer, proposed (and described in detail) in [12] for measuring the spectrum of individual XFEL laser pulses, can successfully be used on SR sources even under steady-state conditions. Along with the monochromator spectrum, one can study changes in the emission spectrum, arising near the absorption edge in different materials (EXAFS and XANES methods) under short-term external impact on a sample.

An accurate theory of this spectrometer was developed. It was shown that a compound X-ray lens forms a secondary source of coherent divergent radiation with desired properties at its focus. The possibility of calculating theoretically the interference pattern for

monochromatic radiation increases the accuracy in determining the emission spectrum from experimental data.

Note that this spectrometer has a relatively simple design, because it consists of standard elements (silicon single crystal, standard compound refractive lens, and standard CCD detector) that are widely used in third-generation SR sources.

ACKNOWLEDGMENTS

REFERENCES

1. N. Kato and A. R. Lang, Acta Crystallogr. **12**, 787 (1959).

2. N. Kato, Acta Crystallogr. **14**, 526 (1961).

3. N. Kato, J. Appl. Phys. **39**, 2225 (1968).

4. A. M. Afanas'ev and V. G. Kohn, Fiz. Tverd. Tela **19**, 1775 (1977).

5. V. G. Kohn, Kristallografiya **24** (4), 712 (1979).

6. V. V. Aristov, V. I. Polovinkina, I. M. Shmyt'ko, and E. V. Shulakov, Pis'ma Zh. Eksp. Teor. Fiz. **28**, 6 (1978).

7. V. V. Aristov, V. I. Polovinkina, A. M. Afanas'ev, and V. G. Kohn, Acta Crystallogr. A **36**, 1002 (1980).

8. V. V. Aristov, V. G. Kohn, V. I. Polovinkina, and A. A. Snigirev, Phys. Status Solidi A **72**, 483 (1982).

9. V. D. Koz'mik and I. P. Mikhailyuk, Pis'ma Zh. Eksp. Teor. Fiz. **28**, 673 (1978).

10. V. G. Kohn, I. Snigireva, and A. Snigirev, Phys. Status Solidi B **222**, 407 (2000).

11. E. V. Shulakov and I. A. Smirnova, Poverkhnost, No. 1, 76 (2001).

12. V. G. Kohn, O. Y. Gorobtsov, and I. A. Vartanyants, J. Synchrotron Radiat. **20**, 258 (2013).

13. A. Snigirev, V. Kohn, I. Snigireva, and B. Lengeler, Nature **384** (6604), 49 (1996).

14. B. Lengeler, C. Schroer, J. Tummler, et al., J. Synchrotron Radiat. **6**, 1153 (1999).

15. http://wwwo.physik.rwth-aachen.de/fileadmin/user_upload/www_physik/Institute/Inst_2B/Gruppe_Lengeler/Praesentation_in_grenoble_july2010.pdf.

16. V. G. Kohn, Poverkhnost, No. 5, 32 (2009).

17. V. G. Kohn, J. Synchrotron Radiat. **19**, 84 (2012).

18. http://kohnvict.ucoz.ru/acl/acl.htm.

Translated by Yu. Sin'kov